Fractal and statistical characterization of brushstroke on paintings

Maxence Bigerelle, Robin Guibert, Anna Mironova, Frederic Robache, Raphaël Deltombe, Ludovic Nys, Christopher Brown

Fractal and statistical characterization of brushstroke on paintings

Maxence Bigerelle[1,2], Robin Guibert[1,3], Anna Mironova[1], Frederic Robache[1], Raphael Deltombe[1], Ludovic Nys[4] and Christopher A Brown[5]

[1] Univ. Polytechnique Hauts-de-France, CNRS, UMR 8201 - LAMIH - Laboratoire d'Automatique de Mécanique et d'Informatique Industrielles et Humaines, F-59313 Valenciennes, France
[2] INSA Hauts-de-France, F-59313 Valenciennes, France
[3] Univ. Lille, CNRS, Centrale Lille, UMR 9013 - LaMcube - Laboratoire de Mécanique Multiphysique Multiéchelle, F-59000, Lille, France
[4] Univ. Polytechnique Hauts-de-France, LARSH - Laboratoire de Recherche Sociétés & Humanités, F-59313 Valenciennes, France
[5] Surface Metrology Laboratory, Mechanical and Materials Engineering Department, Worcester Polytechnic Institute, Worcester, MA 01609-2280, United States of America

E-mail: robin.guibert@uphf.fr

Keywords: roughness, topography, surface metrology, artistic painting, decomposition, painting analysis

Abstract

Identification of an individual artist's touch on paintings is studied using surface metrology. Paintings' topographies were measured using focus variation and stitching, creating 13 × 13 mm maps with 1 μm sampling intervals, and 169 megapixels, with a 10X objective lens. Topographic characterization parameters were analyzed for their ability to differentiate different painters' renderings. Statistical treatments from data mining were used to discriminate, by optimization, multiscale topographic signatures characterized by a multitude of areal texture parameters. It appears that a fractal dimension can define 3 characteristic scale ranges. One from 3 to 70 μm corresponds to brushstroke details. Another, from 70 to 700 μm, corresponds to the topography of the material of the canvas fabric. Finally, scales greater than 700 μm correspond to undulations of the canvas. For scales less than 50 μm, the fractal structure of the topography left by brushstrokes follows a power law characterized by the slopes of the topography. The topography of the clouds painted on the canvas has an Sdq (topographic slopes) increasing with the clarity of the clouds at scales of 3–500 μm. According to the Torrance-Sparrow theory, the higher the Sdq, the more diffuse the light on the surface. The painter therefore wanted to show, by his brushstroke, that the light clouds diffuse more light giving an impression of local brightness. This study is confirmed by the analysis of the painting of Max Savy, a French painter from Carcassonne (1918–2009), which was measured with a white light interferometer Zygo NewView 7300, a X100 objective lens giving a 517 μm × 517 μm stitched surface, with a sampling interval of 0.109 μm. The box-counting method for estimating the fractal dimension of the topography of an oil painting appears optimal by the fact that it morphologically integrates scale variations of the local slopes of the surface morphology. This method thus characterizes the multiscale aspects, as well as the scale changes, of the topography.

1. Introduction

Scientific analysis of artistic paintings has recourse to numerous investigative techniques [1–3]. A number of modern techniques are used to investigate the works of art used for attribution of paintings [4], and art fraud [5] for example. Several kinds of material interactions have been used: raking light [6], infrared imaging [7], ultraviolet fluorescence [8], x-ray methods [9], neutron activation [10], acoustic imaging [11], and thermographic imaging [12]. These aid restorations by providing an in-depth view of paintings. They are also used for authentication, but not primarily to analyze the aesthetics, the painter's touch, or the emotions felt by the painter. They also do not study elementary geometric forms, i.e., topographic features, like those resulting from discrete fundamental brush-stroke-paint-substrate interactions that form topographies on paintings combinations of which lead a complete impression of the art. We can consider three types of sensory information: colors, shapes of regions, and the topographies, i.e., structures or morphologies, of the brushstrokes [13, 14].

The measurement and analysis of topographies is surface metrology, which has origins in engineering design. Surface metrology has expanded into analyses in archaeology [15–18], paleontology, forensics, cultural preservation [19], and art [20, 21]. A particularly interesting commonality of these studies is that their topographies have important, irregular components that cannot be well characterized by conventional geometry. In the last decades of the 20th century high-speed, digital computing facilitated measurement and analysis of topographic irregularities. Concurrently computers enabled visualization and application of Mandelbrot's fractals. Concepts from fractal geometry helped to elucidate and characterize irregular geometries in nature, including roughness, which he called beautiful.

Value in surface metrology can come from discovering strong functional correlations and confident discriminations [22]. Functional correlations can be between topographies and the processing variables that have created them, or between performance and the topographies that influence it. Discrimination means being able to discern, or differentiate, topographies what were created or that perform differently. The ability to create these kinds of value depends on four principles, inclusion of pertinent scales, characterization of pertinent geometric features, acquisition of sufficiently good measurement data, and application of appropriate statistical analyses. The first two, relating to scales and characterizations, are axiomatic for surface metrology. The second two, measurement and statistics follow directly as corollaries. In a review it was found that research, which provided value through discoveries of strong functional correlations or confident discriminations tended to have these four principles in common [23].

The scales, i.e., sizes, spatial frequencies or wavelengths, that are pertinent for solving a particular problem, or for understanding a certain phenomenon, are often not known in advance. Therefore, multiscale regressions, and discrimination tests are used on multiscale geometric characterizations, topographic measurements to determine the pertinent scales. Topographic measurements are inherently multiscale. They contain ranges of scales from a measurement's resolution to a measurement's field of view, or an overall size of stitched measurements. The lower limits of a measurement's resolution is a function of the interactions between an instrument's sensors and the measurands, as well as a measurement system's interpretation of signals from its sensors to estimate heights, sampled at locations on surfaces.

Heights cannot be measured at a point and all the heights on a surface cannot be known. Measured topographies sample heights (z) in a regular spatial array (x, y). Height samples in topographic measurements are determined over sampling zones spaced at sampling intervals in x and y. Other terms for sampling interval are found in the literature, such as, pixel size or measurement interval. Sampling interval is currently used in international and national standards (ISO 25178 [24], ASME B46.1 [25]) and is used here. It is difficult to determine the actual resolution of a measurement instrument on a particular surface, often is it taken to be the sampling interval, which is a lower limit on the resolution.

Multiscale geometric characterizations can be achieved through progressive filtering of topographic data then performing analyses, or by characterizing geometric properties that inherently vary with scales of observation or calculation on irregular surfaces, like slope, area, and curvature. Filtering and use of geometric evaluations that are functions of scale can be used together as is done here.

Paintings' topographies can be considered as collections of topographic features at progressively finer scales. Brushstrokes can be considered collections of ridges left by individual hairs or bristles. There are features on the ridges, some due to constituents in the paints, and to drying and aging phenomena. Some could be due to vibrations and movements during strokes, maybe even from sounds and voices in a painter's studio during a brush stroke. This kind of reductionism applied to topographies can lead to formulation of discrete interaction hypotheses for studying of topographic interactions [22]. Fundamental discrete interactions produce the finest scale topographic features. Larger features and topographies are agglomerates of these fine scale features. This concept provides a useful perspective for considering multiscale formation processes for topographies.

Here, techniques are also investigated in the fields of image analysis and colorimetry. Shugrina *et al* [26] show, by using computer graphics to substitute brushstrokes of different textures on paintings representing the same object, that a viewer's feelings are fully different. Brushstrokemorphologies can be used to classify portrait miniatures [27]. The introduction of brushstrokes textures, called stroke processes [28] on a digitized image, creates non-photorealistic visualization of objects by controlling the color, shape, size and orientation of individual brushstrokes [29]. Brushstrokes textures make the visualization of artistic paintings aesthetically pleasing, by adding morphological information to the original color information of the masterpiece [30]. By introducing biomechanical aspects, it was shown that brush elasticity plays a major role [31] and helps to create a novel painting system with an intuitive haptic interface [32]. It was then proven that forces at the scale of the stroke, linked to friction and viscosity rheology of the paint, must be considered to understand formation of paintings morphologies. An important fact is that stroke morphology can be dissociated from the color. Flagg and Regh show [33], using a projector-guided painting, that pigment and strokes selections can be decomposed to create a multi-layer complex structure. In fact, Li *et al* [34]

make it clear that Van Gogh's work can be analyzed by statistics only of brushstrokes and their shape provided that their numbers are sufficient. This analysis of the morphology of the brushstrokes is sufficient to distinguish Van Gogh's painting in different time periods [34]. The role of complex brushstroke morphology is confirmed by Berezhnoy *et al* [35]. They show that the main spatial characteristics are the brushstroke patterns and their associated orientation distribution [35]. From Li *et al* [34], the discriminating brushstrokemorphology is the number of brushstrokes in a neighborhood. This can be obtained simply by counting the brushstrokes in a neighborhood, and noting sizes, lengths, and broadness of the brushstrokes, as well as their broadness homogeneity, straightness, elongation and orientation. This clearly shows that morphologies are complex, even if brushstrokes can be modeled by derived surfaces such as cubic b-spline [36] or Bezier interpolation [37]. The effect of strokes seems to be multiscale [38]. Hertzmann [39] showed that a series of spline brushstrokes is required to a create realistic painting. Hendriks, from the Van Gogh museum and Hughes from Princeton University [40] define the characteristic touch of the painter Vincent Van Gogh at the scale of the brushwork described by different sizes of wavelets present in digital images. This wavelet analysis confirms that discriminating aspects of paintings can be based on analyses of complex brushstroke structures on paintings' black and white digitalized images based on photographs [41].

Hertzmann [42] presents a technique for simulating the physical appearance of brushstrokes under lighting, supposing that paintings are composed of a list of brushstrokes. A height map is assigned to each stroke and the topographic map for the painting is produced by rendering the brushstrokes' textures. The final painting is rendered by combining the painting's colors with the height map. However, nothing is explained on how to obtain the heights of the surface topography, which seems to be simulated, nor on the illumination model on the rough surface. This makes this approach appear as a non-realistic rendering tool of a photo. However, the author shows that by playing with the illumination angles that the appearance of the photo changes markedly, due to the introduction of the height amplitude map. This point is particularly made by Elkhuizen *et al* [43] that compare three multiscale, 3D scanning techniques: 1) optical coherence tomography, 2) 3D scanning based on fringe-encoded stereo imaging (at two resolutions), and 3) 3D digital microscopy. These methods are applied to analyze the surface topology of 'Girl with a Pearl Earring' painted by Johannes Vermeer. Elkhuizen *et al* [43] write a paragraph that we discuss, that clearly distinguishes photography analyses used by the computer and image analyses community:

'*Paintings are generally considered in terms of their (2D) depiction, but the physical artwork also has a third dimension. The substrate is rarely completely flat, and subsequent paint and varnish layers also influence the surface topography. This effect can be intentional—using the paint to create a 3D effect—or the consequence of drying, hardening, or degradation. Artists, including Vermeer, deliberately created 3D textural effects on the surface. For instance, they used impasto to create additional reflections for highlights, or used 3D effects to emphasize the textural appearance of the material they were depicting. Alternatively, three-dimensional brushstrokes can be the consequence of a fast-paced, expressive style*' Elkhuizen *et al* 2019 [43].

The surface metrology interacts with the physical science community (rheology, optics, scattering, etc.). The associated mathematics for metrology is close to geostatistics, and an environment/material model for the physical sciences. There are few articles on the use of 3D techniques. Consider the recent bibliography of Elkhuizen *et al* on 3D techniques with 16 articles, which in fact is limited to 11 [44–54]. According to our research, this appears to be a state of the art with only the reference [55] added. This number is small compared to the consequent number of publications devoted to the image analysis of artistic paintings. Moreover, in the 11 publications, the authors never treat the painter's touch from a 3D surface topography point of view. Therefore, it seems that the microscopic aspects in 3D topography measurements are not treated. However, Elkhuizen *et al* [43] find that the 3D digital microscopy based on focus variation and the multiscale optical coherence tomography offer the highest measurement accuracy and precision. However, the small field-of-view of focus variation makes them relatively slow to investigate larger areas of paintings. We propose to summarize in a table the advantages and disadvantages of the two techniques: 3D topography versus photography (table 1).

In this paper, the main purpose of surface topography studies is to organize information through physical interpretations. The fundamental problem is to answer the following questions 'Is a fractal dimension a relevant parameter?' and 'At which scale does it characterize an artist' style?' These questions have no meaning if not 'relevant to a physical process'. Let us illustrate this point by an example of surface characterization from a topographic measurement. Painted areas, p, were made by the same painter. Topographic measurements were made on regions (similar reasoning would be applicable to surface characterization by image analysis). Having these topographic measurements, the common use is to deduce some parameters (for example, the Sa, St, Sq, etc from ISO 25178-2 [24]). We are looking for a correlation between these few parameters and different parts of a painting. For example, it may be usual to use a particular topographic characterization parameter (often Sa or St) and to analyze the relations of this parameter with dynamics of the painter and then to deduce possible characteristics specific to this work. However, if another parameter better characterizes the surface in

Table 1. Advantages and drawbacks of 3D topography compared to imaging techniques used for artistic painting studies.

Criteria	Topographic map	Images map
Acquisition		
Existence of available database	Database does not exist.	Numerous existing databases but often with different shooting conditions and resolutions
Acquisition speed	Slow digital acquisition.	Quick photo shooting
Apparatus mobility	Difficult to transport. Requires an adapted assembly.	Portable, 'standard' tripods
Influence of environment over acqusition	Expansion control because long measurement, vibration-free environment, thermal control…	Almost instantaneous measurements
Dimension of field of view	Small investigated area, impossibility of full measurement of the picture	Integral measurement with lower resolution
Working distance	Needs to be close to the painting (briefly, from 0.5 mm to 10 mm depending on the optics and the measurement method)	Measure quite far from the pictorial support
Caution about the integrity of measurement object	Precaution to be taken not to touch the painting, do not put a too intense luminous flux.	No danger
Stitchability	Many measurements must be stitched, made difficult by the irregularity of the topographies.	Easier stitching by using the optical characteristics of the lenses (parallax, lens distortion,)
Quality of acquisitions	Good quality color image at high resolutions in high precision z-stacks. [56] (Focus variation microscope).HDR Mode [57]	Medium resolution, almost no stacking required. Low macro depth of field.HDR mode possible
Control over light conditions	Use of several light sources on a ring. Constant luminous flux [58]	Lighting conditions more delicate to control
File data encoding	32-bit topographic encoding [59]	Often file encoded on 16 bits (grey levels) or 16 bits per channel (color images)
Possibility to use multiple lights	Can take measurements at different angles of illumination with high precision for defect detection.	Multi-light analysis requires heavy on-site installation.
Presence of quality map	Quality map possible [60]	No quality Map.
Help with algorithmic classification		
Data diversity usefulness	Has 3 maps: Quality map, topographic, and image. Facilitates future shape detection algorithms [61] (Focus variation microscope).	Algorithms often based only on color/grayscale image detection
Help in the analysis of the painter's touch, specific approach to topography		
Possibility to analyse rheology of the paint	Can help to understand the rheology of the paint that forms the topography	Impossible
Inclusion of pigment scales	Can include pigment scales [62, 63]	Impossible
Superposition of topographic maps and images	Using focus variation illumination algorithms, we can recreate the photographic images and analyze the renderings sought by the painter. [64] (Focus variation microscope)	Impossible
Possibility to interpret biomechanical aspect of the painting process	Easier interpret biomechanical aspects of painters by integrating the deformation of the paint using mechanics of materials [65]	It is limited to simplistic mechanical models of mass spring type in the x-y plane.
Ability of evaluate damages	Adept at quantifying morphologies of different damages (cracks, chemical changes, protusions, local deformations, …). [66]	Can only detect visual defects at a medium scale and eventually a count of these defects.
Represent reflectivity of the painting	Allows for creation of BRDF (Bidirectional Reflectance Distribution Function) / BTF (Bidirectional Texture Function) for computer graphics based on topography [67, 68].	Requires heavy RTI type mounting.

relation to the painter's description, the conclusions of the analysis must be qualified, or even different. Similarly, it is common practice in the scientific community to use a topographic characterization parameter which has a known physical interpretation. Topographic slopes characterized as Sdq (slope, ISO 25178-2 [24], root mean square gradient of the surface) can be indicative of gloss. However, if it is shown experimentally that another topographic characterization parameter better characterizes this physical phenomenon, then its discriminating character must be justified. Therefore, to test the efficiency of a topographic characterization parameter, a measure of relevance must be constructed and applied to the totality of these parameters. This approach has never been undertaken in the field of artistic painting of surface

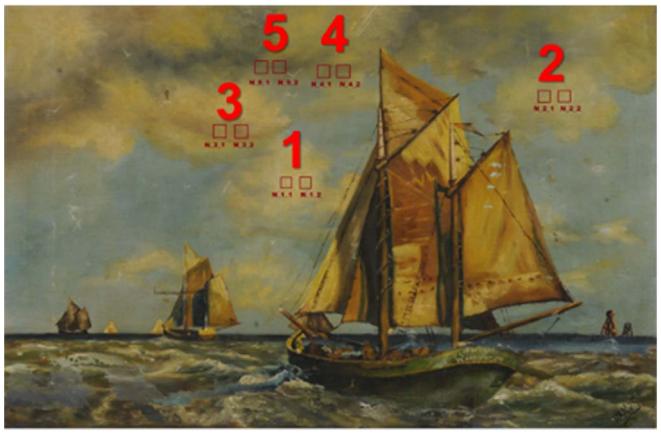

Figure 1. The Boat from Vlaardingen (920 × 730 mm), near La Hague in Holland painted presumably by Josephus Gerardus Hans (or Hanns). Artwork stated to be in the public domain. The red squares (inside different clouds) correspond to regions on which topographic analyses are carried out.

states and is the keystone of this article. It requires calculation of parameters listed in the standards and the bibliography. It is necessary to create a robust method of measurement relevant to the physical system. In our case, all topographic characterization parameters are analyzed and assigned an efficiency number for ranking of their relevance according to their efficiency index. This philosophy of numerical treatments of surface states frees us from subjectivity (i.e., assumptions about roughness parameter relevancy before the study) in the use of these parameters and to treat measurements with more objectivity. By this method, we will show that a fractal dimension is a relevant parameter with respect to the description of the work. Also, this article focuses on the analysis of factual quantitative data (roughness), which is one component among others, such as colors, in paintings. This kind of factual and quantitative data is useful to describe the artist's intention about how a painting should look like (visual appearance), and is separated from how people perceive a painting, or how people feel about it, which needs a more subjective study.

2. Materials and methods

2.1. Painting 'Fishing boats in the North Sea'

In order to analyze the topography of an oil painting, we selected a work containing several identical motifs (boats, clouds, waves) in order to look for topographic differences and commonalities in these motifs. This oil painting (figure 1), in a rather poor state of conservation, represents several sailing fishing boats on a turbulent sea with greenish waters, not far from a coast without relief, where two high towers with wooden structures can be discerned on the right. These boats with auric rigging are perfectly identifiable. They were ketches, medium-sized, two-masted sailing ships, the largest of which was located forward. Ketches were used in Holland for fishing from the 17th to early 20th century, particularly for herring. The vessel in the foreground has on its stern the name of its home port, Vlaardingen (Flardingue), located west of the port of Rotterdam towards the mouth of the Waal (Rhine). Its reputation was for herring that fishermen of the province of Zuid-Holland sought in the North Sea with these types of vessels. This painting bears a signature with a proper Germanic name, Hanns. Under this spelling, this name seems to be of German origin; however, it was also encountered in the Netherlands in other forms (Haans, Hans). The RKD (Rijksbureau voor Kunsthistorische Documentatie) in The Hague has not been able to identify an artist with this name closer to this painting. A painter from South Holland by the name of Josephus Gerardus Hans, who was born in la Hague in 1826 and died in Ryswyk on 18 July 1891, is mentioned in Emmanuel Bénézit's *Dictionnaire critique et documentaire des peintres* (last edition, 1999, vol. 6, p. 731), but it seems too old for this work that, according to the style and workmanship, one is tempted to date it more from the 1920s or 1930s, or even from the post Second World War period.

2.2. Topographical measurements

Focus variation was used to measure surface topography. This metrological system combines a shallow depth of field and vertical scanning to provide true color topographic data (for image analysis also) from the variation in image sharpness on CCD arrays. The main component of the system consists of a precision optical system, which can be equipped with a variety of lenses, to make measurements at different resolutions. The visual correlation between the color optical image of the part surface and the height information, which are often related to each other and are therefore essential to the analysis of painting surfaces. In our case, an Alicona InfiniteFocusG5 (Raaba/Graz, Austria) is used with a X10 objective lens, over 13 × 13 mm by stitching with sampling intervals of 1 μm,

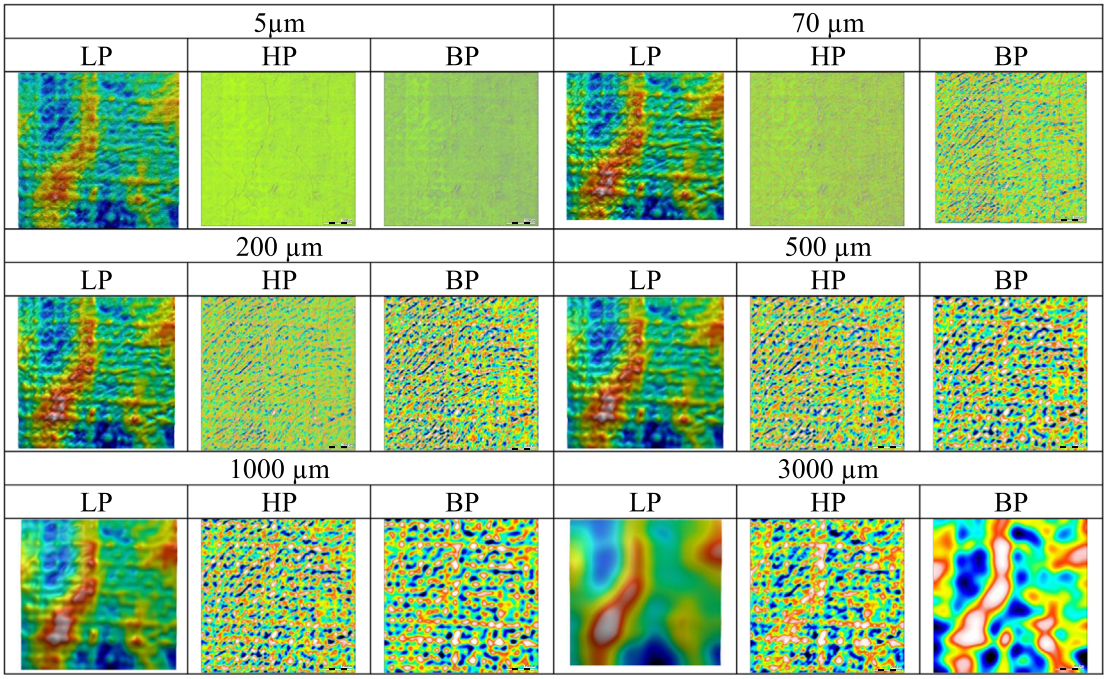

Figure 2. Gaussian filtering examples given cut-off values (along X and Y axes) of 5, 70, 200, 500, 1000 and 3000 μm using high pass (HP) filters, retaining topographic scales finer than cut-off values down to the instrument's resolution, low pass (LP)-filtered surfaces containing topographic scales coarser than cut-off values, and finally band pass (BP) filters that contains topographic scales between cut-off values.

forming a map of 169 megapixels. Two such measurements on five clouds, presenting different brightness aspects were made (see figure 1, from 1 luminous cloud to 5 dark cloud). After measurement, form was removed from the surface using a 3rd order polynomial, non-measured points were filled, and another 3rd order polynomial was used for finding a surface reference plane.

3. Multiscale analysis

3.1. Multiscale decomposition

To determine scales most relevant to a painters' aptitude, multiscale decompositions were conducted. Basically, measured topographies were analyzed using MountainsMap® software. Three Gaussian spatial filters, high pass (HP), band pass (BP), and low pass (LP) filters, were applied to decompose the scales. By applying an HP filter, topographic scales finer than a defined threshold were retained. Conversely, LP filters extracted scales below a defined threshold (figure 2). A band pass filter characterizes topographies between two scales of a decomposition.

3.2. Multiscale topographical graph

By sequentially increasing or decreasing cut-off values, topographical scales were revealed, classical roughness with the HP filter, and waviness with the LP filter and particular details with the BP filter. Then, for each surface of the spectrum, several topographic characterization parameters were calculated. For each of these parameters, its evolution according to the filter cut-off and therefore scale, was obtained.

3.3. Sdq: a discriminating parameter

Basically, these plots describe their multi-scale behavior. A first analysis shows that Sdq describes topographies of the painted surfaces of the five clouds systematically (figure 3).

The Sdq (average slope) roughness parameters represents the mean slope of the surface. It is certain that if the sampling interval (dx pitch) changes on the measurement device, the parameter Sdq is highly likely to change due to the fractal aspect of repeating features at finer scales in the topography. In fact, the calculation of the Sdq parameter is quite close to Mandelbrot's philosophy where 'the yardstick' is represented by the sampling interval (Richardson's method). As the method of calculation from ISO 25178-2 [24] only calculates the Sdq in relation to the sampling interval, i.e., slopes in relation to its closest neighbours. This minimizes the influence of the sampling interval variance between different measurements and gives a constant scale for calculating values of Sdq. Here the sampling interval, dx, is constant at 1.1 μm. This is not perfect, although it estimates a slope by Sdq according to ISO 25178-2. However, in our case, low pass filtering has been performed around 100 μm. At the scales used to calculate the Sdq, sampling intervals are less than the cutoff of the filter, Sdq estimates average topographic slopes, and thus becomes less sensitive to the 'fractal' effects of

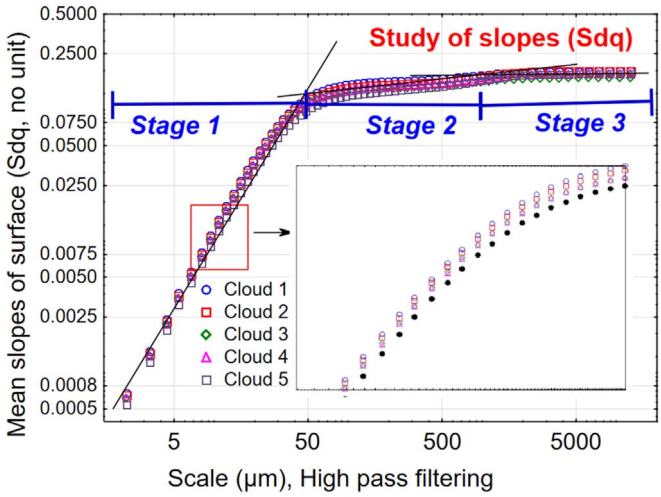

Figure 3. Evolution of slopes, as root mean square gradients, Sdq, at different levels of high pass filtering, i.e., scales, for the five clouds described in figure 1.

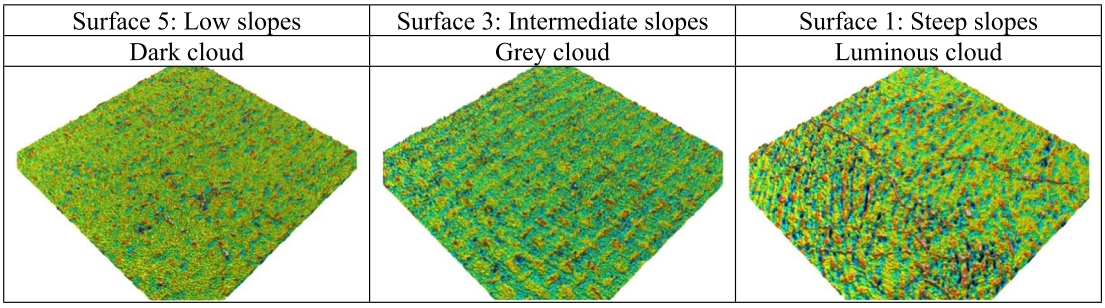

Figure 4. Maps obtained after high pass filtering at a cutoff of 70 μm. The three zones 1, 3, 5 correspond to cloud topography (see figure 1) for three levels of brightness.

slopes changing with scale in these topographies. At first, we can see that this parameter distinguishes 3 regimes:

1. Scaling laws for scales less than 70 μm. This means that the slopes increase with the wavelength. As the length of the filter increases, new peaks are added, increasing average slopes. These additions lead to a fractal-type topography (peaks within peaks etc.) according to a simple scale law of type $Sdq\ \alpha\ \lambda^{\alpha}$ where λ the filter cutoff length and α the scale exponent;
2. Slow increasing of Sdq from 70 to 800 μm, there are no real power laws, this is the end of the fractal regime;
3. Above 800 μm, Sdq is practically constant, slopes no longer increase, and the topography has become stationary with respect to scale.

For the regime 1, there is the following classification whatever the cutoff

$$\mathrm{Sdq}(1) > \mathrm{Sdq}(2) > \mathrm{Sdq}(3) = \mathrm{Sdq}(4) > \mathrm{Sdq}(5),\quad \lambda \in (2;\ 70)\,\mu\mathrm{m} \tag{1}$$

Topographies are expected to be more intricate and torturous as slopes increase. Figure 4 shows three topographies of clouds 1, 3, and 5 after a 70 μm high pass filter. On these three topographies, slopes increase as the topographies become more intricate and tortuous. The dark cloud 5 appears the smoothest with the lowest slopes, while the light cloud 1 has the steepest slopes, and the slopes in the grey cloud 3 are intermediate.

4. Relevance of the topographic characterization parameters

4.1. Principle

For a given spatial scale, there could be topographic characterization parameters that can assist in detecting differences between cloud types. Exceptionally, there could be clouds painted with different colors, which appear different, but have the same topography at the

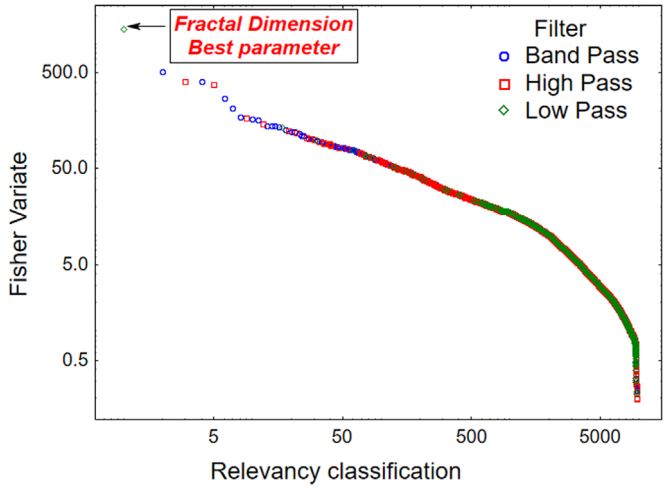

Figure 5. Plot of the relevance graph, i.e., the decrease of F for all parameters computed for all scales with the three filters (BP, HP, and LP).

scales of interest. Statistics are used to test if two or more cloud types are discernible. For this, the F (Fisher-Snedecor) variable from analysis of variance (ANOVA) is an indicator of differences between these five cloud topographies. The value F represents the ratio of the mean variance of topographies introduced by surface structuring divided by the mean variance of measurement of a surface. The methodology for finding the relevant roughness parameters with ANOVA is presented in Deltombe *et al* [69].

The total variance of characterization parameters from the topographic measurements is equal to the sum of the variance between the means of the measurements corresponding to each cloud morphology and the mean variance of the measurement errors. It is then possible to define a so-called Fisher-Snedecor variable F. This is an estimate of a signal-to-noise ratio. The higher F is, the better the ability for the considered roughness parameter to differentiate clouds. If a characterization parameter is unable to see differences between clouds, F values will be close to unity. For more details, see [69] for the formulation, [70] for application in wear, [71] in lubrification, [72] in biology and [73] for coating functionalities. For each roughness parameter at a given scale, F value is computed. It is then possible to find the relevant parameters by plotting the F value against the parameter rank, sorted by F value.

4.2. Results

By plotting the decrease of F (Fisher-Snedecor variable) versus the rank for all parameters, efficacies of parameters to describe the difference between clouds can be displayed (figure 5).

From figure 5, the parameter that stands out without context is the fractal dimension in low pass filtering. Figure 6 then represents the values of the latter for the 5 types of clouds.

This confirms that fractal aspects of the painting discern differences in appearance of the clouds that we showed in figure 3 with their topographic slopes. Curves plotting the evolution of the fractal dimension are identical in appearance. Visually, 3 scale ranges appear which match those shown for the average topographic slopes. This supports the multiscale aspects mentioned earlier: the fractal dimension, being related to the power laws of metric indicator, can deduce changes in these laws. A visual analysis of the decomposition thus seems to show that these three scale ranges correspond to 3 different mechanisms corresponding closely to the regimes defined previously:

3–78 μm: **Brushstroke.** Over these scales, the filtered measurement renderings (figure 6, left) show peaks and valleys that are more or less curved, a sign of a topography left by the painter's brush. The fractal dimension is close to that of Brownian motion, whose theoretical fractal dimension is 2.5. The differences between the different clouds are highly significant over these scales.

78–743 μm: **Canvas Filling.** Over these scales, the filtered images (figure 6, center) show fairly regular patterns whose pitch corresponds to the pitch of the mesh of the canvas. A Fourier transform analysis (figure 7) confirms the periodicity with a peak at 770 μm which represents the end of stage 2. Regime two thus corresponds well to an area between the traces of the brushstroke and the average size of the cells of the textile. This means that it translates the filling rate of these cuvettes as shown in the two topographies included in figure 7.

743–12000 μm: **Canvas geometry.** Identical ripples for all the clouds are found. The fractal dimension tends towards 2 which characterizes a Euclidean surface, i.e., a smooth shape. At these scales, ripples are shown. These are introduced by the tension of the textile fibers which influence the morphology of the

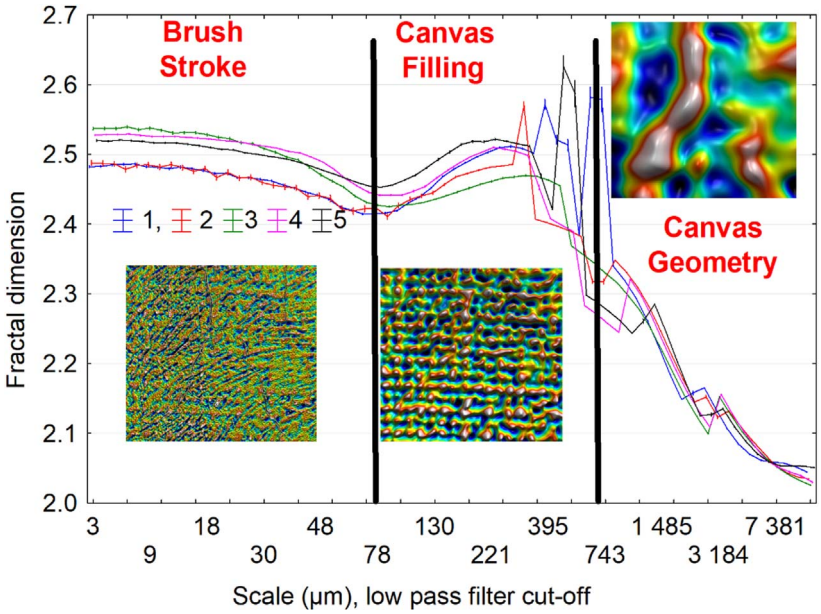

Figure. 6 Evaluation of the fractal dimension at various scales for five cloud regions on the painting.

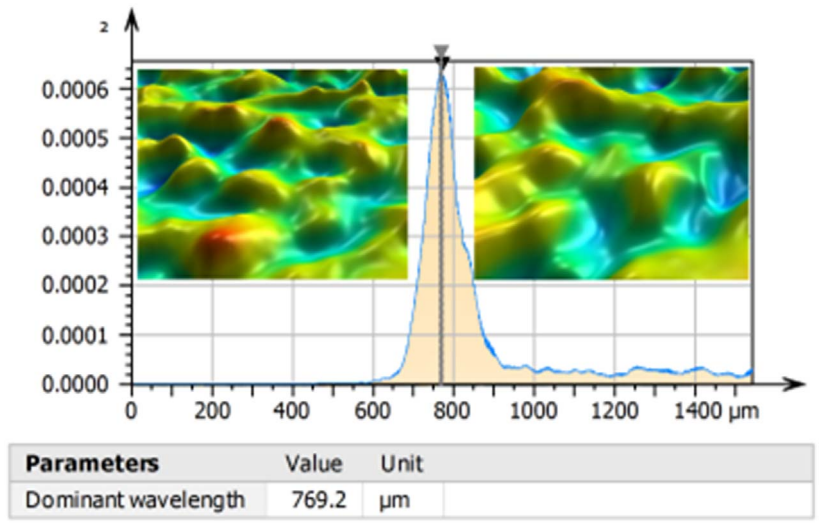

Figure 7. Fourier transform to analyze canvas texturing. The peak around 0.8 mm represents the mesh size of the canvas.

fabric with an amplitude 5 times smaller than the size of the mesh.

5. The fractal aspect of artistic painting: a discussion

Since the early 1960s and thanks to the work of Benoît Mandelbrot [74, 75], fractal analysis provides a special approach to many physical problems. The notion of fractal dimension of a curve is a topological measure recently introduced in various fields of physics (diffusion, fluid mechanics, percolation, fracture, tribology [76, 77]). This dimension characterizes the degree of occupation of the 3D space where the surface evolves. In the case of these types of curves, the fractal dimension is between 2 and 3. A surface with a dimension close to 2 will be fairly 'regular', but if its dimension tends towards 3, it will present a very pronounced 'irregularity'. The formulation and calculation of the fractal dimension of a surface (or curve) are well mastered now from a topological point of view, thanks to the work of Hausdorff [78], Minkowski [79], and Bouligand [80], but its exact numerical calculation remains debatable. There are many methods for calculating the fractal dimension [81–83] (see also ASME B46.1 Ch. 10 [84] and ISO 25178-2 [24] standards) on profiles ($z = z(x)$) and surfaces ($z = z(x, y)$). Some give different results, and some do not lead to expected numerical values when applied to curves of kn own dimensions. Differences can reach 40% of theoretical values.

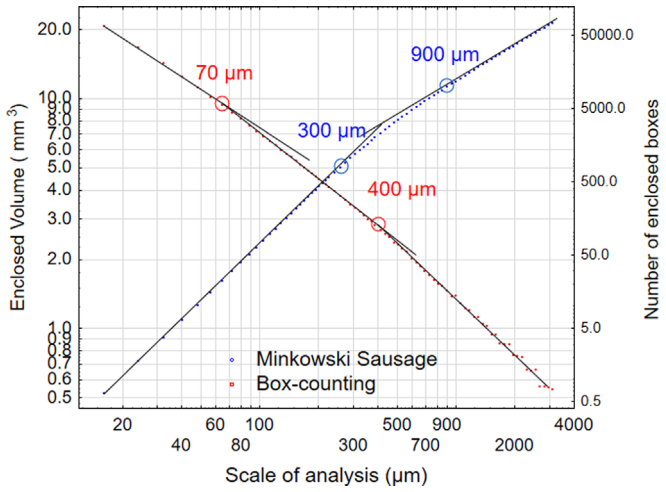

Figure 8. Fractal plot for both methods (box-counting and Minkowski) computed from the surface shown in figure 2.

5.1. Box-counting versus Minkowski sausages

Two fractal dimension calculation methods have been implemented here and classified by relevance to show suitable methods for describing morphologies of topographies on scale ranges in two- and three-dimensional spaces. Efficacy can provide a phenomenological approach to physical interpretations. Two profile methods are used here [74]:

- Box-counting. The fractal dimension calculated by this method is the best parameter considered here to describe the topological particularities of each cloud.
- Bouligand-Minkowski. The fractal dimension calculated by this method is relevant but its ability to describe the topological features of each cloud on all scales is only ranked 30th.

Details of these methods are considered below in order to find the multiscale attributes and topological relationships that unite all these scales by power law analysis.

However, it is possible, apart from fractal dimensions, to assert that a surface has geometric properties of fractals over some scale range and to calculate the exponent of the power law. In fact, real surfaces are never purely fractal as Mandelbrot mentions in his seminal article 'How Long is the Coast of Britain'. The method that Mandelbrot describes uses line segments, whose lengths correspond to scales of observation, to measure systematically apparent lengths of the coast as functions of scale. It is also known as coastline, Richardson or compass method and has been applied to measured profiles [82] and extended to surfaces with virtual triangular tiling [83]. At sufficiently fine scales, fractal dimensions can change because these methods can become sensitive to aspects of geometric features not observed at larger scales. In the case of artistic painting, we think that the lower scale is close to the size of the pigments.

The box-counting method leads to a log-log plot (figure 8) which has three straight linear parts whereas the Minkowski method has only two, with a linearity deviation between 300 and 900 μm. Box-counting seems to detect the power laws more clearly, which gives it the advantage of detecting the regimes of the multiscale morphology of the painting more clearly.

Three regimes appear in the log-log plot of the Sdq diagram (figure 3) that correspond to what we identified as brushstroke, 3–78 μm, canvas filling, 78–743 μm, and canvas geometry, 743–12000 μm (see figure 6). Box-counting appears to distinguish the fractal aspect of the brushstroke around 50 μm, given by Sdq (figure 3). Minkowski does not detect a crossover between regimes at this scale, overestimating it at 300 μm. With box-counting, the local box $N(\tau, x_i)$ counted in x_i with width τ is in fact strongly related to the local slope of the surface $Sdq(\tau, x_i)$. In x_i with width τ by the approximate average relationship is $Sdq(\tau, x_i) \cong \tau \dfrac{N(\tau, x_i)}{\tau} = N(\tau, x_i)$. The second threshold in box-counting, at 400 μm, corresponds to half the wavelength value of the mesh of the textile canvas $= \dfrac{\lambda_{canvas}}{2} = \dfrac{769}{2} \cong 400\ \mu$m (see the power spectrum figure 7). This critical length detected by box-counting corresponds to the average width of the peaks and valleys of the region defined by the mesh and the number of boxes. It represents a rate of filling valleys and paint covering on the projected area τ^2 of a volume $\tau^3 N(\tau, x_i)$. Consider that the more negative the slopes of the log-log diagram are, the more the surface is disordered, and the higher the fractal dimension. For box-counting, with slopes of $-\Delta$, and Δ the fractal dimension of the surface, then $\Delta_{BrushStroke} < \Delta_{CanvasMesh} < \Delta_{CanvasForm}$. Box-counting for estimating the fractal dimension of the topography of an oil painting appears optimal because it

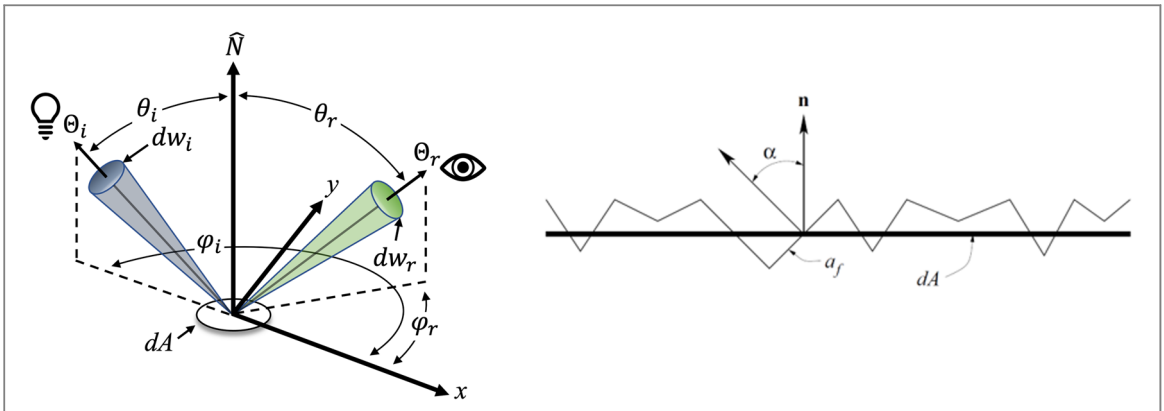

Figure 9. 'Bidirectional Reflectance Distribution Function' BRDF expressed in terms of viewing and illumination angles where polar angle θ (rad), azimuth angle φ (rad), irradiance E (Wm^{-2}), radiance L ($Wm^{-2}Sr^{-1}$), radiant flux Θ (W), solid angle $d\omega$ (Sr), surface element V (m^2) as in [89], a_f is the area of each micro-facet [88].

morphologically integrates the scale variations of the local slopes of the surface morphology. Box-counting characterizes multiscale aspects as well as scale changes of the topography.

6. Optical analysis of light reflection on painted surfaces

The goal of this section is to try to find a possible correlation between the Sdq, representing the mean slope of the surface, and the nature of light reflection. Here, Sdq is treated as a parameter computed (globally or locally) on a scale-limited topography. Cloud topography has an Sdq, slope, increasing with cloud clarity in the 3–500 μm scale range. Torrance and Sparrow and Shipulski and Brown [85] have developed raytracing models based on geometric optics for light reflection on irregular surfaces using slopes [86]. These models neglect the electromagnetic wave nature of light. Raytracing is valid only if the irregularities of the surface are much greater than the wavelength of the source, and express incident radiance scattered to a camera sensor by a surface patch. These raytracing models are based on representing topographies by micro-facets. Each facet is described by an angle between its normal and the normal to the macroscopic datum plane, ***n***. If we assume the surface is isotropic, the distribution of the facet normals is rotationally symmetrical with respect to ***n***. The slope distribution can then be modeled by a one-dimensional function, such as a normal distribution of zero mean and standard deviation σ_α. Modeling of reflection using microfacets and the laws of geometrical optics thus leads to a model with only one specular lobe. This result is expected since the laws of geometrical optics are only valid for irregular surfaces. Torrance and Sparrow add a Lambertian term to their reflection equation and apply it for the reflectance in computer graphics [87] which becomes:

$$I(\theta_i, \theta_r, \alpha, \sigma_\alpha) = \kappa_{diff} L_i dw_i \cos(\theta_i) + \kappa_{spec} \frac{L_i dw_i}{\cos(\theta_r)} e^{-\frac{\alpha^2}{2\sigma_\alpha^2}} \quad (2)$$

where α, L_i and dw_i represent respectively the angle between the surface normal and the facet of the surface, the radiance of the source, and the solid angle under which the surface patch sees the source. The surface is illuminated (see figure 9) by the incident beam that lies on the (y, z) plane with a polar angle of θ_i and a particular reflected beam which we are interested in travels along the direction θ_r (more exactly (θ_r, φ_r)). The constant κ_{spec} represents the specular reflection coefficient and κ_{diff} represents the coefficient of diffuse reflection (or Lambertian) (see [88] for details).

This model 'Bidirectional Reflectance Distribution Function' BRDF model is widely used [90, 91] to describe illumination of surface in image synthesis such as raytracing [92], reflectance in uncalibrated photometric [93], estimating model parameters from images by a six-color camera [94] and is intensively used in computer graphics [95]. Chen [89] shows experimentally that this model is well adapted to describe vanished painted samples showing brush marks.

Figure 10 shows how the slopes can be locally calculated from the topographic map, either by calculating the local values of Sdq in square sub-regions (scale is the length of the box side: 35 μm), either by calculating the slope in square sub-regions (also at 35 μm scale).

While the clarity of the clouds increases with the slopes of the surface (Sdq), the higher the Sdq, the more the specular component decreases and thus the Lambertian component becomes more preponderant according to the Torrance-Sparrow theory (equation (2)). Larger Sdqs, cause more diffuse reflection from the surface. Painters can show, by a brushstroke, that the light clouds diffuse more light, giving an impression of local brightness, avoiding a dark and obscuring climate to the painting.

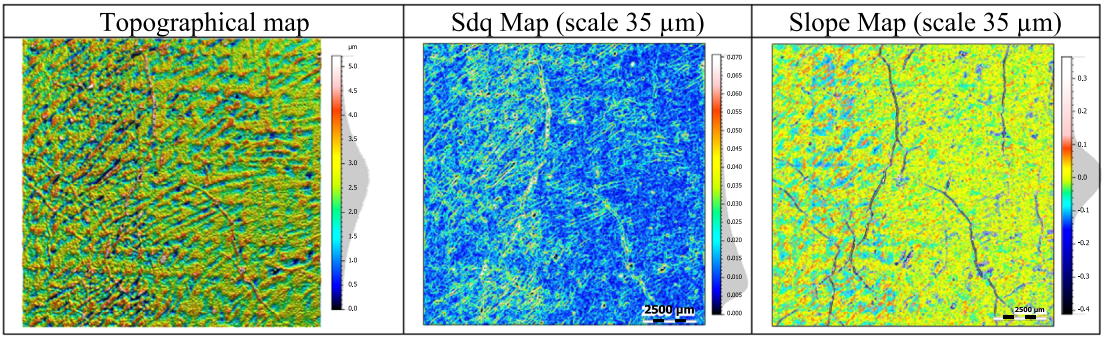

Figure 10. Topographic map, Sdq map and slope map of a cloud from the painting.

7. Validation of the slope hypothesis on a painting by Max Savy

7.1. The painter

Born in Albi in 1918, Max Savy arrived in the Aude in 1936. He left his mark on Aude painting first of all through his role as a teacher. Teacher, professor of drawing at the Ecole Normale, he gave his lessons to generations of Carcassonnais. Then, Max Savy devoted himself entirely to his art. Great painter but also excellent draftsman, illustrator and engraver, his career is international. The golden ochres, browns and greens that characterize his paintings magnify the landscapes of les Corbières, so dear to his heart, making some say that he was the 'Peintre des Corbières'. Max Savy in his works thus retraces everyday life: he paints scenes where the characters, tiny peasants, are gleaners, bent towards the Earth with small white pebbles, often dominated by black trees surrounding them. However, the painter has known several periods, and his canvases are a real success. From the end of the war, 'Les Savy' are displayed by the most famous galleries, in the whole of Europe and then the United States. In 2009, he lost his eyesight and stopped painting. He would die slowly on October 30, 2010 a few months after being made a Knight of the Legion of Honor. The previously presented methodology is tested on a Max Savy's painting, ≪Bâteau de pêche au port≫. This painting shows a boat near a deck, where small houses are located. This painting is set at a Sunset, which accentuates blue and orange colors. Details such as a lighthouse, gulls and other boats are displayed in the background. The reflection of the sky can be observed in the sea.

7.2. Topographic measurement, relevance and statistical analysis

We are going to reproduce the same method of analysis of Savy's painting as that of Hanns, namely the role of topography on the sensory impression left by the diffusion of clouds. This painting is quite interesting in terms of luminosity. Indeed, Max Savy played on two effects: a fog effect in the distance reinforced by a twilight aspect and a reflection of the clouds on the water surface which gives an additional strengthening aspect of the diffusion effect desired to show that the sea has waves (visible in the foreground). A white light interferometer (NewView 7300, ZYGO, USA) equipped with a X100 objective was used for the topography measurements. Two regions are studied: one for the sky and one for the sea. Colorimetric maps of the approximative studied regions are shown in figures 11(a) and (b). Inside those approximative regions, random locations in a 2×2 cm area are selected, representing respectively cloud and reflected cloud on the sea. 100 measurements, 517×517 μm, were made with sampling intervals of 0.109 μm using stitching. Fifty-one roughness parameters were computed based on standards. These included amplitude parameters, functional parameters, spatial parameters, hybrid parameters, including root-mean square gradient, i.e., slope, Sdq, and feature parameters using surface segmentation. Then, the relevance protocol described in section 4.a was applied and relevance graph is plotted (figure 11(g) on the top right). Slope, Sdq, is the best parameter to discriminate the sky and the reflected sky on the sea. Thanks to a bootstrap protocol [96], the probability density function of the mean Sdq value can be plotted to appreciate the relevancy (figure 11(h) on the bottom right). Unambiguously, the Sdq corresponding to the sky area is lower than the Sdq of its projection on the sea.

7.3. Confirmation of slope assumptions

The slope hypothesis is that slopes could discriminate different types of brushstrokes. Here, Sdq is computed over the whole scale range of the topography, i.e., on the unfiltered topography. The sea has a higher Sdq (1.37) than the sky (1.20). According to the Torrance-Sparrow theory, the higher the Sdq, the more light diffuses on the surface. The painter wanted to show, by his brushstroke, that the sea diffuses the reflection of the Sun on the wavelet of the sea, giving an impression of mist that highlights the foreground. Therefore, the slope hypothesis is applicable for this painting.

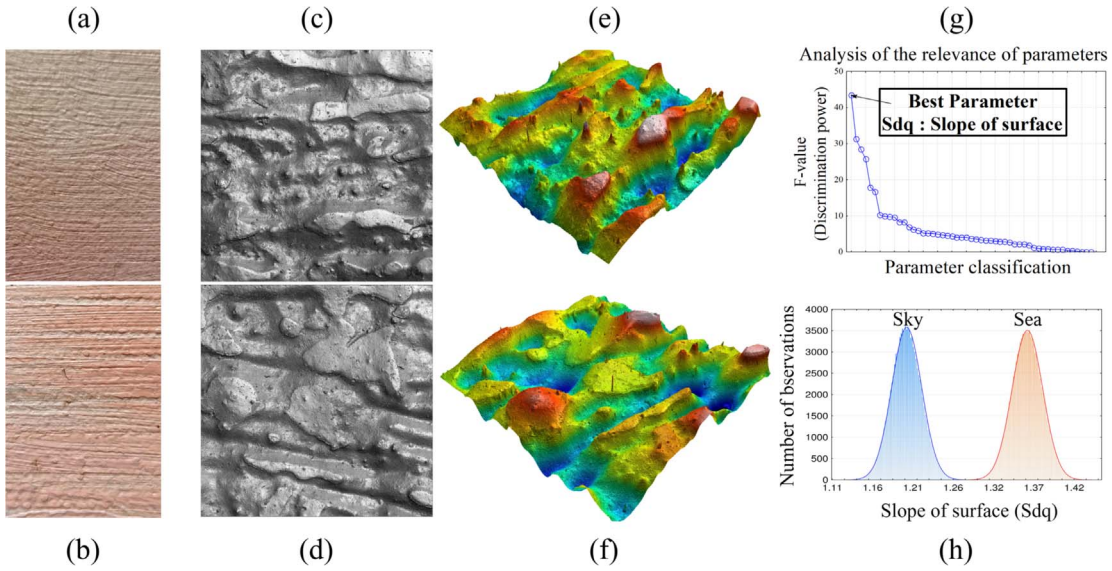

Figure 11. Graphical abstract of the analysis of the Max Savy's oil painting. Various maps of the painting are displayed: full colorimetric maps of the approximative regions of the sky (a) and the sea (b), reflectance maps of the sky (c) and the sea (d), topographic maps of the sky (e) and the sea (f). An analysis of the relevance of parameters (g) shows that Sdq is the best parameter discriminating the sky and the sea, as seen in histogram (h).

8. Discussion about perception of paintings by observers

There are multiples ways to look at a painting. While it is true that people looking at a painting use both non-subjective data (color, topography) and subjective data (interpretation of the painting, subjective perception of a painting features), each can be studied separately. This article focuses on non-subjective data (topography and brightness, which is linked to slopes of the topography), but they are only some components of a painting among others, such as colors, which are useful to detect objects in paintings. What we described as artist's intention in this article is the intention about how a painting looks like, with factual data like color, roughness and reflectance maps using Bidirectional Texture Function (BTF). No assumptions are made about how the painting is perceived by observers nor how they feel after looking at the painting. However, other authors worked on the perception of a painting, such as Taylor *et al* [97] that shows how people perceived brushstrokes orientations on painting images. For brushstrokes made from left to right, most people perceive the movements correctly while other perceive it from right to left. Also, Amirshahi *et al* [98] and Hayn-Leichsenring *et al* [99] proposed two subjective studies about paintings and how participants evaluate if a painting is aesthetic or pleasurable to view, which show aesthetics and individual liking are not necessarily linked. Therefore, roughness parameters, which can give information about the painting aesthetic value, and how people perceive paintings as pleasurable might not be as correlated. Further works are then necessary to assess roughness influence over subjective perception of paintings.

9. Conclusions

There are still many challenges to be addressed. Surface metrology can be compared with texture indications obtained by illumination of the surface and the many models cited in the references in the field of cultural heritage. A major challenge is creating methods for high-resolution imaging of a painting, isolation of objects that compose it, and measurements of each object by automatic repositioning and adapted stitching.

Topographic measurement and analyses, surface metrology, provide new perspectives for understanding a painter's touch. Some of these measurements cannot be made over an entire painting. Surface metrology, once limited to local analyses of the damage for future restoration, offer a new investigation on sensory perception scales thanks to new stitching techniques [100] to cover larger regions.

By analyzing the result of ANOVA and Fisher-Snedecor value, the Sdq roughness parameter has been identified as the most relevant parameter. Results were then focused on Sdq, but other roughness parameters could also be relevant. Brushstrokes on the paintings present a fractal structure, which can be characterized by the parameter of the slope, Sdq, which discriminates the different morphological structures of a painting.

Relevant topographic characterization parameters are related to slopes on the surface. The topographic measurements therefore are sufficient to model light reflection, except of course the colorimetric measurements which are beyond our scope here.

Perspectives are opened to associate biomechanical actions of a painter, including the rheology of the paint materials, to address the techniques painters use

to obtain optical effects with the surface. The fractal dimension of the surface topography at the brush-stroke scale is a relevant parameter: painters' styles are multiscale. However, it is necessary to filter to extract the different components inherent to different physical phenomena.

This would require a high-precision instrumented bench, an optimized acquisition and an optimized processing of roughness parameters on a surface with a sinuous contour (i.e., not rectangular).

ORCID iDs

Maxence Bigerelle https://orcid.org/0000-0002-4144-245X
Robin Guibert https://orcid.org/0000-0002-2656-2840
Frederic Robache https://orcid.org/0000-0003-0547-4873
Ludovic Nys https://orcid.org/0000-0003-2518-518X

References

[1] Fleming S J 1976 *Authenticity in Art: the Scientific Detection of Forgery* (London: Inst. of Physics)
[2] Taft W S, Mayer J W, Newman R, Stulik D and Kuniholm P 2000 *The science of paintings* (New York: Springer)
[3] Murashov D M 2015 Feature description of informative fragments in the problem of computerized attribution of paintings *Pattern Recognit Image Anal.* **25** 692–704
[4] Shchegoleva N L and Vaulina Y A 2019 Use of digital technology for the attribution of paintings *Computational Science and Its Applications—ICCSA 2019 Lecture Notes in Computer Science* ed S Misra *et al* (Cham: Springer International Publishing) 11622, 792–801
[5] Ragai J 2013 The scientific detection of forgery in paintings *Proc. Am. Philos. Soc.* **157** 164–75
[6] Murashov D M, Berezin A V and Ivanova E Y 2019 Measuring parameters of canvas texture from images of paintings obtained in raking light *J. Phys. Conf. Ser.* **1368** 032024
[7] Delaney J K, Zeibel J G, Thoury M, Littleton R, Palmer M, Morales K M, Rie E R de la and Hoenigswald A 2010 Visible and infrared imaging spectroscopy of picasso's *harlequin musician* : mapping and identification of artist materials *in Situ Appl. Spectrosc.* **64** 584–94
[8] Pelagotti A, Pezzati L, Piva A and Del A 2006 Mastio 2006 multispectral UV fluorescence analysis of painted surfaces *14th European Signal Processing Conf.* pp 1–5
[9] Neelmeijer C and Mäder M 2002 The merits of particle induced X-ray emission in revealing painting techniques *Nucl. Instrum. Methods Phys. Res. Sect. B Beam Interact. Mater. At.* **189** 293–302
[10] Cotter M J, Meyers P, Zelst L and Sayre E V 1973 Authentication of paintings by Ralph A. Blakelock through neutron activation autoradiography *J. Radioanal. Chem.* **15** 265–85
[11] Zhang H, Sfarra S, Saluja K, Peeters J, Fleuret J, Duan Y, Fernandes H, Avdelidis N, Ibarra-Castanedo C and Maldague X 2017 Non-destructive investigation of paintings on canvas by continuous wave terahertz imaging and flash thermography *J. Nondestruct. Eval.* **36** 34
[12] Gavrilov D, Maev R G and Almond D P 2014 A review of imaging methods in analysis of works of art: Thermographic imaging method in art analysis *Can. J. Phys.* **92** 341–64
[13] Sablatnig R, Kammerer P and Zolda E 1998 Hierarchical classification of paintings using face- and brush stroke models *Proc. Fourteenth Int. Conf. on Pattern Recognition (Cat. No.98EX170)* vol 1 (Brisbane, Qld.: IEEE Comput. Soc.) pp 172–4
[14] Sablatnig R, Kammerer P and Zolda E 1998 Structural analysis of paintings based on brush strokes *Scientific Detection of Fakery in Art* ed W McCrone, D R Chartier and R J Weiss (San Jose, CA) (*Event: Photonics West '98 Electronic Imaging*) 3315, 87–98
[15] Stemp W 2002 Documenting stages of polish development on experimental stone tools: surface characterization by fractal geometry using UBM laser profilometry *J. Archaeol. Sci.* **0** 287–96
[16] Stemp W 2014 A review of quantification of lithic use-wear using laser profilometry: a method based on metrology and fractal analysis *J. Archaeol. Sci.* **48** 15–25
[17] Stemp W, Watson A and Evans A 2015 Surface analysis of stone and bone tools *Surf. Topogr.: Metrol. Prop.* **4** 013001
[18] Stemp W J, Macdonald D A and Gleason M A 2019 Testing imaging confocal microscopy, laser scanning confocal microscopy, and focus variation microscopy for microscale measurement of edge cross-sections and calculation of edge curvature on stone tools: preliminary results *J. Archaeol. Sci. Rep.* **24** 513–25
[19] Ravines P, Chen J and Wichern C M 2010 Surface characterization and monitoring of surface changes after conservation treatments of silver gelatin photographic papers using confocal microscopy *Scanning* **32** 122–33
[20] Artal-Isbrand P and Klausmeyer P 2013 Evaluation of the relief line and the contour line on Greek red-figure vases using reflectance transformation imaging and three-dimensional laser scanning confocal microscopy *Stud. Conserv.* **58** 338–59
[21] Artal-Isbrand P and Klausmeyer P 2015 Using reflectance transformation imaging and 3D laser scanning confocal microscopy to evaluate relief and contour lines on ancient attic greek vases *Microsc. Today* **23** 30–5
[22] Brown C A 2021 Surface metrology principles for snow and ice friction studies *Front. Mech. Eng.* **7** 753906
[23] Brown C A *et al* 2018 Multiscale analyses and characterizations of surface topographies *CIRP Ann* **67** 839–62
[24] ISO 25178-2 2012 *Geometrical Product Specifications (GPS) — Surface texture: areal — Part 2: terms, definitions and surface texture parameters* (International Organisation for Standardization)
[25] ASME 2002 B46.1Standard - Surface Texture, surface roughness, waviness and lay *Am. Soc. Mech. Eng. Am. Natl. Stand.* **1–98**
[26] Shugrina M, Betke M and Collomosse J 2006 Empathic painting: interactive stylization through observed emotional state *Proc. of the 3rd international symposium on Non-photorealistic animation and rendering - NPAR '06* (Annecy: ACM Press) p 87
[27] Melzer T, Kammerer P and Zolda E 1998 Stroke detection of brush strokes in portrait miniatures using a semi-parametric and a model based approach *Proc.. Fourteenth Int. Conf. on Pattern Recognition (Cat. No.98EX170)* vol 1 (Brisbane, Qld.: IEEE Comput. Soc) pp 474–6
[28] Zhao M and Zhu S-C 2011 Customizing painterly rendering styles using stroke processes *Proc. of the ACM SIGGRAPH/ Eurographics Symp. on Non-Photorealistic Animation and Rendering - NPAR '11* (Vancouver, British Columbia: ACM Press) p 137

[29] Haeberli P 1990 Paint by numbers: abstract image representations *Proc. of the 17th annual conference on Computer graphics and interactive techniques - SIGGRAPH '90* (Dallas, TX: ACM Press) pp 207–214
[30] Healey C G, Tateosian L, Enns J T and Remple M 2004 Perceptually based brush strokes for nonphotorealistic visualization *ACM Trans. Graph.* **23** 64–96
[31] Lee J 1999 Simulating oriental black-ink painting *IEEE Comput. Graph. Appl.* **19** 74–81
[32] Baxter B, Scheib V, Lin M C and Manocha D 2001 DAB: interactive haptic painting with 3D virtual brushes *Proc. of the 28th annual conference on Computer graphics and interactive techniques - SIGGRAPH '01 (ACM Press) pp 461–468*
[33] Flagg M and Rehg J M 2006 Projector-guided painting *Proc. of the 19th annual ACM symposium on User interface software and technology - UIST '06* (Montreux: ACM Press) p 235
[34] Li J, Yao L, Hendriks E and Wang J Z 2012 Rhythmic brushstrokes distinguish van gogh from his contemporaries: findings via automated brushstroke extraction *IEEE Trans. Pattern Anal. Mach. Intell.* **34** 1159–76
[35] Berezhnoy I E, Postma E O and van den Herik H J 2009 Automatic extraction of brushstroke orientation from paintings: POET: prevailing orientation extraction technique *Mach. Vis. Appl.* **20** 1–9
[36] Pham B 1991 Expressive brush strokes *CVGIP, Graph. Models Image Process.* **53** 1–6
[37] Siong C Y 1990 Bézier brushstrokes *Comput.-Aided Des.* **22** 550–5
[38] Hertzmann A 2003 A survey of stroke-based rendering *IEEE Comput. Graph. Appl.* **23** 70–81
[39] Hertzmann A 1998 Painterly rendering with curved brush strokes of multiple sizes *Proc. of the 25th annual conference on Computer graphics and interactive techniques - SIGGRAPH '98* (ACM Press) pp 453–460
[40] Hendriks E and Hughes S 2009 Art, Conservation and Authenticities; Material, Concept, Context *Van Gogh's brushstrokes: Marks of Authenticity?* ed E Hermens and T Fiske (Archetype) 143–52
[41] Johnson C, Hendriks E, Berezhnoy I, Brevdo E, Hughes S, Daubechies I, Li J, Postma E and Wang J 2008 Image processing for artist identification *IEEE Signal Process Mag.* **25** 37–48
[42] Hertzmann A 2002 Fast paint texture *Proc. of the second international symposium on Non-photorealistic animation and rendering - NPAR'02* (Annecy: ACM Press) p 91
[43] Elkhuizen W S, Callewaert T W J, Leonhardt E, Vandivere A, Song Y, Pont S C, Geraedts J M P and Dik J 2019 Comparison of three 3D scanning techniques for paintings, as applied to Vermeer's 'Girl with a Pearl Earring' *Herit. Sci.* **7** 89
[44] Blais F *et al* 2005 Ultra-high resolution imaging at 50 μm using a portable XYZ-RGB color laser scanner *International Workshop on Recordingg, Modeling, and Visualization of Cultural Heritage* (Ascona: CRC Press) 1–16
[45] Blais F, Taylor J, Cournoyer L, Picard M, Borgeat L, Godin G, Beraldin J-A, Rioux M and Lahanier C 2007 Ultra high-resolution 3D laser color imaging of paintings: the Mona Lisa by Leonardo da Vinci *The 7th Int. Conf. on Lasers in the Conservation of Artworks [Proc.] NRC Publications Archive / Archives des publications du CNRC (Madrid, Spain: CRC Press) pp 1–8*
[46] Factum Arte 2016 *Lucida—Discovering an Artwork through Its Surface* (Madrid, Spain: Technical Report. Factum Foundation)
[47] Del Sette F, Patané F, Rossi S, Torre M and Cappa P 2017 Automated displacement measurements on historical canvases *Herit. Sci.* **5** 21
[48] Akca D, Grün A, Breuckmann B and Lahanier C 2007 High definition 3D-scanning of arts objects and paintings *Optical 3 -D measurement techniques VIII* ed A Gruen and H Kahmen (Zurich, Switzerland: ETH Zurich) pp 50–8
[49] Karaszewski M, Adamczyk M, Sitnik R, Michoński J, Załuski W, Bolewicki P and Bunsch E 2013 Automated full-3D Digitization system for Documentation of paintIngs *Optics for Arts, Architecture, and Archaeology IV* ed L Pezzati and P Targowski (Munich, Germany) (*SPIE Optical Metrology*) 8790, pp 1–11
[50] Zaman T 2013 *Development of a Topographic Imaging Device For The Near-Planar Surfaces of Paintings Thesis* Delft University of Technology
[51] Zaman T, Jonker P, Lenseigne B and Dik J 2014 Simultaneous capture of the color and topography of paintings using fringe encoded stereo vision *Herit. Sci.* **2** 23
[52] Palma G, Pingi P, Siotto E, Bellucci R, Guidi G and Scopigno R 2019 Deformation analysis of leonardo da Vinci's 'adorazione dei magi' through temporal unrelated 3D digitization *J. Cult. Herit.* **38** 174–85
[53] Cacciari I, Nieri P and Siano S 2014 3D digital microscopy for characterizing punchworks on medieval panel paintings *J. Comput. Cult. Herit.* **7** 1–15
[54] van den Berg K J, Daudin M, Joosten I, Wei B, Morrison R and Burnstock A 2008 A comparison of light microscopy techniques with scanning electron microscopy for imaging the surface of cleaning of paintings *9th Int. Conf. NDT Art Jerus. Isr.* 25–30
[55] Liang H, Lucian A, Lange R, Cheung C S and Su B 2014 Remote spectral imaging with simultaneous extraction of 3D topography for historical wall paintings *ISPRS J. Photogramm. Remote Sens.* **95** 13–22
[56] Wu A, Shi Y, Lu R and Zhang Z 2020 Sequence image registration for large depth of microscopic focus stacking *IEEE Access* **8** 6533–42
[57] Piper J 2010 Software-based stacking techniques to enhance depth of field and dynamic range in digital photomicrography *histology protocols methods in Molecular Biology* 611 ed T D Hewitson and I A Darby (Totowa, NJ: Humana Press) pp 193–210
[58] Tian L, Wang J and Waller L 2014 3D differential phase-contrast microscopy with computational illumination using an LED array *Opt. Lett.* **39** 1326
[59] ISO 25178-71: 2017 (en) Geometrical product specifications (GPS) — Surface texture: Areal — Part 71: Software measurement standards
[60] Newton L, Senin N, Gomez C, Danzl R, Helmli F, Blunt L and Leach R 2019 Areal topography measurement of metal additive surfaces using focus variation microscopy *Addit. Manuf.* **25** 365–89
[61] Fontana R, Gambino M C, Greco M, Marras L, Materazzi M, Pampaloni E, Pezzati L and Poggi P 2003 Integrating 2D and 3D Data for Diagnostics of Panel Paintings *Optical Metrology for Arts and Multimedia* ed R Salimbeni (Munich, Germany) (*Optical Metrology*) 5146, 88–98
[62] Doménech-Carbó A, Doménech-Carbó M T and Mas-Barberá X 2007 Identification of lead pigments in nanosamples from ancient paintings and polychromed sculptures using voltammetry of nanoparticles/atomic force microscopy *Talanta* **71** 1569–79
[63] Pereira C, Ferreira I M P L V O, Branco L C, Sandu I C A and Busani T 2013 Atomic force microscopy as a valuable tool in an innovative multi-scale and multi-technique non-invasive approach to surface cleaning monitoring *Procedia Chem.* **8** 258–68
[64] Daffara C, Fontana R, Melchiorre Di Crescenzo M, Scrascia S and Zendri E 2011 Optical techniques for the characterization of surface-subsurface defects in painted layers(Munich, Germany) 8084p80840X
[65] Tiennot M, Paardekam E, Iannuzzi D and Hermens E 2020 Mapping the mechanical properties of paintings via nanoindentation: a new approach for cultural heritage studies *Sci Rep.* **10** 7924
[66] Pawlak A, Skrzeczanowski W and Czyż K 2017 LIBS, optical and multivariate analyses of selected 17 th-century oil paintings from the Museum of King Jan III's palace at Wilanów *Proc. of the Int. Conf. LACONA XI* (Torun: Nicolaus Copernicus University Press) 191–204
[67] Elkhuizen W S, Zaman T, Verhofstad W, Jonker P P, Dik J and Geraedts J M P 2014 *Topographical Scanning and*

Reproduction of Near-Planar Surfaces of Paintings ed M V Ortiz Segovia *et al* (San Francisco, CA) 9018 p 901809
[68] Elkhuizen W S, Essers T T W, Lenseigne B, Weijkamp C, Song Y, Pont S C, Geraedts J M-P and Dik J 2017 Reproduction of Gloss, Color and Relief of Paintings using 3D Scanning and 3D Printing *Eurographics Workshop Graph. Cult. Herit.* 183–7
[69] Deltombe R, Kubiak K J and Bigerelle M 2014 How to select the most relevant 3D roughness parameters of a surface: Relevance of 3D roughness parameters *Scanning* **36** 150–60
[70] Garabedian C, Vayron R, Bricout N, Deltombe R, Anselme K and Bigerelle M 2020 *In vivo* damage study of different textured breast implants *Biotribology* **23** 100133
[71] Tchoundjeu S, Bigerelle M, Robbe-Valloire F, Da Silva Botelho T and Jarnias F 2020 How to select 2D and 3D roughness parameters at their relevant scales by the analysis of covariance *Materials* **13** 1526
[72] Bigerelle M, Giljean S and Anselme K 2011 Existence of a typical threshold in the response of human mesenchymal stem cells to a peak and valley topography *Acta Biomater.* **7** 3302–11
[73] Anselme K and Bigerelle M 2006 Effect of a gold–palladium coating on the long-term adhesion of human osteoblasts on biocompatible metallic materials *Surf. Coat. Technol.* **200** 6325–30
[74] Mandelbrot B 1967 How long is the coast of britain ? Statistical self-similarity and fractional dimension *Science* **156** 636–8
[75] Mandelbrot B 1975 *Les Objets Fractals : Forme, Hasard et Dimension* (Paris: Flammarion)
[76] Gouyet J F 1992 *Physique et Structures Fractales* (Paris: Masson)
[77] Mehaute L 1992 *Les Géométries Fractales* (Paris: Hermès)
[78] Hausdorff F 1919 Dimension und äusseres mass *Math. Ann.* **79** 157
[79] Minkowski H 1901 Uber die begriffe länge, oberfläche und volumen, jahr.deut *Math* **9** 115–21
[80] Bouligand G 1935 *Les définitions modernes de la dimension* (Paris: Hermann)
[81] Dubuc B, Quiniou J F, Roques-Carmes C, Tricot C and Zucker S W 1989 Evaluating the fractal dimension of profiles *Phys. Rev. A* **39** 1500–12
[82] Brown C A and Savary G 1991 Describing ground surface texture using contact profilometry and fractal analysis *Wear* **141** 211–26
[83] Brown C A, Charles P D, Johnsen W A and Chesters S 1993 Fractal analysis of topographic data by the patchwork method *Wear* **161** 61–7
[84] ASME B46.1 2009 Surface Texture (Surface Roughness, Waviness, and Lay)
[85] Shipulski E M and Brown C A 1994 A scale-based model of reflectivity *Fractals* **02** 413–6
[86] Torrance K E and Sparrow E M 1967 Theory for off-specular reflection from roughened surfaces *J. Opt. Soc. Am.* **57** 1105
[87] Cook R L and Torrance K E 1981 A reflectance model for computer graphics *ACM SIGGRAPH Comput. Graph.* **15** 307–16
[88] Park J and N. DeSouza G 2005 3-D modeling of real-world objects using range and intensity images *Machine Learning and Robot Perception Studies in Computational Intelligence* ed B Apolloni *et al* (Berlin, Heidelberg: Springer) 7, pp 203–64
[89] Chen Y 2008 Model Evaluation and Measurement Optimization for the Reproduction of Artist Paint Surfaces through Computer Graphics Renderings *Master of Science dissertation, Rochester Institute of Technology* (https://scholarworks.rit.edu/theses/8242/)
[90] Nicodemus F E 1970 Reflectance nomenclature and directional reflectance and emissivity *Appl. Opt.* **9** 1474
[91] Whitehouse D J, Bowen D K, Venkatesh V C, Lonardo P and Brown C A 1994 Gloss and surface topography *CIRP Ann.* **43** 541–9
[92] Meister G, Wiemker R, Monno R, Spitzer H and Strahler A 1998 Investigation on the torrance-sparrow specular brdf model *IGARSS '98. Sensing and Managing the Environment. 1998 IEEE International Geoscience and Remote Sensing. Symposium Proceedings. (Cat. No.98CH36174)* (Seattle, WA: IEEE) 4, pp 2095–7
[93] Georghiades 2003 Incorporating the Torrance and Sparrow model of reflectance in uncalibrated photometric stereo *Proc. Ninth IEEE Int. Conf. on Computer Vision* vol 2 (Nice: IEEE) pp 816–23
[94] Tanaka N, Tominaga S and Kawai T 2000 Estimation of the Torrance-Sparrow reflection model from a single multi-band image *Proc. 15th Int. Conf. on Pattern Recognition* vol 3 (Barcelona: IEEE Comput. Soc) pp 596–9
[95] Kurt M and Edwards D 2009 A survey of BRDF models for computer graphics *ACM SIGGRAPH Comput. Graph.* **43** 1–7
[96] Najjar D, Bigerelle M and Iost A 2003 The computer-based bootstrap method as a tool to select a relevant surface roughness parameter *Wear* **254** 450–60
[97] Eric T, Taylor J, Witt J K and Grimaldi P J 2012 Uncovering the connection between artist and audience: Viewing painted brushstrokes evokes corresponding action representations in the observer *Cognition* **125** 26–36
[98] Amirshahi S A, Hayn-Leichsenring G U, Denzler J and Redies C 2015 Jenaesthetics subjective dataset: analyzing paintings by subjective scores *Computer Vision - ECCV 2014 Workshops Lecture Notes in Computer Science* ed L Agapito *et al* (Cham: Springer International Publishing) 8925, pp 3–19
[99] Hayn-Leichsenring G U, Lehmann T and Redies C 2017 *Subjective Ratings of Beauty and Aesthetics: Correlations With Statistical Image Properties in Western Oil Paintings -Percept* **8** 204166951771547
[100] Lemesle J, Guibert R and Bigerelle M 2023 A Novel 3D topography stitching algorithm based on reflectance and multimap *Appl. Sci.* **13** 857